SUPPORTING INFORMATION

Pyrazino[2,3-f][1,10]phenanthroline-Based Color-Tunable Thermally Activated Delayed Fluorescent Emitters with AIE characteristics for High-Efficiency Organic Light-Emitting Diodes.

Pratima Yadav,[a] Sunil Madagyal,[a] Aniket Chaudhari,[a] Gokul Ganesan,[b] Guan-Yu Su,[c] Yi-Ting Chen,[c] Prabhakar Chetti,[d] Chih-Hao Chang,[c] Shantaram Kothavale,[e]* Atul Chaskar[a]**

[a]*Department of Chemistry, Institute of Chemical Technology, Mumbai, N.P.Marg., Matunga, Mumbai-400019, Maharashtra, India.*

[b]*National Centre for Nanosciences & Nanotechnology, University of Mumbai, Vidyanagari, Mumbai-400098, Maharashtra, India.*

[c]*Department of Electrical Engineering, Yuan Ze University, Taoyuan 32003, Taiwan*

[d]*Department of Chemistry, National Institute of Technology, Kurukshetra, India.*

[e]*School of Chemistry, The University of Edinburgh, Edinburgh EH9 3FJ, United Kingdom.*

**Corresponding author: chc@saturn.yzu.edu.tw, ac.chaskar@ictmumbai.edu.in*

Table of contents.

SI-1 Experimental procedures

Methods and Materials

All the required chemicals and solvents were purchased from Sigma-Aldrich and BLD Pharma Ltd. All the Photophysical measurements were carried out using 10μM solutions. These solutions were prepared with HPLC grade solvents purchased from Sigma-Aldrich. Thermal measurements up to 600^{o}C were carried out using HITACHI STA7300 instrument at a rate of 10^{o}Cmin^{-1}under nitrogen atmosphere. Electrochemical analysis was done using Metrohm Autolab PGSTAT204 147 Potentiostat/Galvanostat in cyclic voltammetry mode. The electrode systems used were silver/silver chloride (Ag/AgCl) as a reference, a Platinum wire electrode as a counter, and glassy carbon electrode as a working electrode. Indium tin oxide (ITO)-coated glass and commercial organic materials were purchased from Shine Materials Technology.

Device fabrication and characterization of OLED's

Indium tin oxide (ITO)-coated glass and commercial organic materials were purchased from Shine Materials Technology. Organic materials were subjected to temperature-gradient sublimation in a high vacuum before use. The ITO substrate was washed in sequence with deionized water and acetone, followed by treatment with plasma. The bottom-emitting OLEDs were fabricated using ITO as the anode, followed by the deposition of multiple organic layers, topped by a metal cathode layer. The organic and metal layers were deposited by thermal evaporation in a vacuum chamber with a base pressure of < 10^{-6} Torr. Device fabrication was completed in a single cycle without breaking the vacuum. The deposition rates of organic materials and aluminium were respectively kept at around 0.1 and 0.5 nm/s. The active area was defined by the shadow mask (2 × 2 mm^2). Current density-voltage-luminance characterization was done using two Keysight B2901A current source-measure units equipped with a calibrated Si-photodiode. The electroluminescent spectra of the devices were recorded using an Ocean Optics spectrometer.

SI-2 Experimental (synthesis)

Synthesis of [1,2-bis(4-(3,6-di-tert-butyl-9H-carbazol-9-yl) phenyl) ethane-1,2-dione] (2)

4,4'-Dibromobenzil (1 g, 2.717 mmol) was reacted with 3,6-di-tert-butyl-9H-carbazole (1.669 g, 5.98 mmol), Cs_2CO3 (2.655 g, 8.151 mmol), $Pd(OAc)_2$ (122 mg, 5 mol%) and tri-tert-butyl phosphine (219.88 mg, 1.086 mmol) in anhydrous toluene in inert nitrogen environment. The resulting mixture was stirred at 110 ℃ for 12 hr. The reaction mixture was poured in ice cooled water and was extracted with dichloromethane and dried over anhydrous Na_2SO_4. The organic layer was concentrated on rotary evaporator and purified through column chromatography (1:1 DCM: hexane). Yellow coloured solid was obtained (1.26 g, 61.0%) which was confirmed using ^{1}H NMR and HRMS.

^{1}H NMR (500 MHz, $CDCl_3$) δ 8.29 (d, *J* = 8.6 Hz, 4H), 8.14 (d, *J* = 1.1 Hz, 4H), 7.82 (d, *J* = 8.6 Hz, 4H), 7.50 (s, 8H), 1.47 (s, 36H). **MS:** m/z 765.4400 [$(M+H)^+$]

Synthesis of [1,2-bis(4-(9,9-dimethylacridin-10(9H)-yl) phenyl) ethane-1,2-dione] (3)

4,4'-Dibromobenzil (1 g, 2.717 mmol) was reacted with 9,9-dimethyl-9,10-dihydroacridine (1.25 g, 5.978mmol), Cs_2CO_3 (2.655 g, 8.151 mmol), $Pd(OAc)_2$ (122 mg, 5 mol%) and tri-tert-butyl phosphine (219.88 mg, 1.086 mmol) in anhydrous toluene in inert nitrogen environment.

The resulting mixture was stirred at 110 ℃ for 12 hr. The reaction mixture was poured in ice cooled water and was extracted with dichloromethane and dried over anhydrous Na_2SO_4. The organic layer was concentrated on rotary evaporator and purified through column chromatography (1:1 DCM: hexane). Yellow coloured solid was obtained (1.08 g, 63.7%) which was confirmed using ^{1}H NMR and HRMS.

^{1}H NMR (500 MHz, $CDCl_3$) δ 8.25 (d, *J* = 8.4 Hz, 4H), 7.55 (d, *J* = 8.4 Hz, 4H), 7.49 (dd, *J* = 7.4, 1.4 Hz, 4H), 7.07 – 6.99 (m, 8H), 6.50 (d, *J* = 7.8 Hz, 4H), 1.67 (s, 12H). **MS**: m/z 625.2846 [$(M+H)^+$]

Synthesis of [1,2-bis(4-(10H-phenoxazin-10-yl) phenyl) ethane-1,2-dione] (4)

4,4'-Dibromobenzil (1 g, 2.717 mmol) was reacted with phenoxazine (1.094 g, 5.978 mmol), in Cs_2CO_3 (2.655 g, 8.151 mmol), $Pd(OAc)_2$ (122 mg, 5 mol%) and tri-tert-butyl phosphine (219.88 mg, 1.086 mmol) anhydrous toluene in inert nitrogen environment. The resulting mixture was stirred at 110 ℃ for 12 hr. The reaction mixture was poured in ice cooled water and was extracted with dichloromethane and dried over anhydrous Na_2SO_4. The organic layer was concentrated on rotary evaporator and purified through column chromatography (1:1 DCM: hexane). Yellow coloured solid was obtained (0.97 g, 62.3%) which was confirmed using ^{1}H NMR and HRMS.

^{1}H NMR (500 MHz, DMSO) δ 8.26 (d, *J* = 8.4 Hz, 4H), 7.71 (d, *J* = 8.5 Hz, 4H), 6.81 (dd, *J* = 7.6, 1.7 Hz, 4H), 6.77 – 6.69 (m, 8H), 6.05 (dd, *J* = 7.7, 1.6 Hz, 4H). **MS:** m/z 573.1798 [$(M+H)^+$].

Synthesis of 5,6-diamino-1,10-phenanthroline from 1,10-phenanthroline

Synthesis of 1,10-phenanthroline-5,6-dione

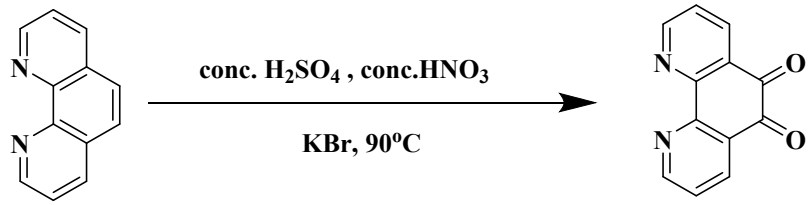

Scheme S1a. Synthesis of 1,10-phenanthroline-5,6-dione.

A mixture of 1,10-phenanthroline (2.0 g) and KBr (2.0 g) was taken in a flask. 30 ml mixture of concentrated sulphuric acid and concentrated nitric acid (2:1) precooled in ice bath for 20 mins was taken in a dropping funnel was added to the reaction mixture dropwise. The oil-water separator was connected to the flask and the mixture was heated to 90 ℃ for 8 hr. The cooled mixture was poured in ice water and neutralised using 30% NaOH solution till pH 6-7 was achieved. The organic compound was extracted using dichloromethane, dried over anhydrous Na_2SO_4. The organic layer was concentrated using rotary evaporator giving orange yellow coloured crude product with a yield of 78.38%. The crude product was recrystallised using 95% ethanol.

Synthesis of (5E,6E)- 1,10-phenanthroline-5,6-dioxime.

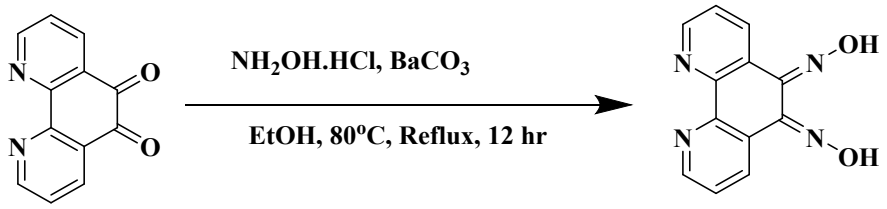

Scheme S1b. Synthesis of (5E,6E)- 1,10-phenanthroline-5,6-dioxime.

A mixture of 1,10-phenanthroline-5,6-dione (1.68 g, 7.99 mmol) was dissolved in 50 ml ethanol and $NH_2OH{\cdot}HCl$ (1.944 g, 27.97 mmol), $BaCO_3$ (2.368 g, 11.967 mmol) were added to it. The mixture was refluxed overnight at 83℃ with constant stirring. The reaction mixture was first evaporated over rotary evaporator and solid residue was treated with 160 ml of 0.2M HCl and stirred for 30 mins. The reaction mixture was filtered through vacuum pump and washed with excess water, ethanol and diethyl ether. A yield of 81.25 % was achieved. The light-yellow coloured 1,10-phenanthroline-5,6-dioxime product was dried in vacuum oven for at 80 ℃ for 12 hr.

Synthesis of 1,10 phenanthroline-5,6-diamine.

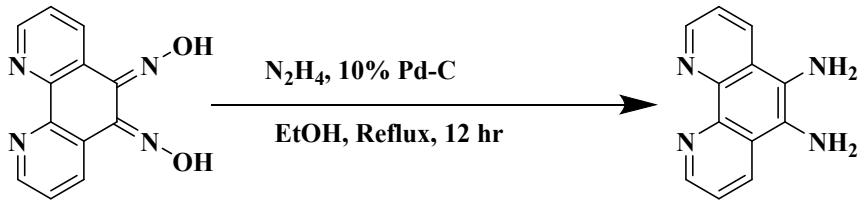

Scheme S1c. Synthesis of 1,10 phenanthroline-5,6-diamine.

A slurry of 2 g of 1,10-phenanthroline-5,6-dioxime and 2g of Pd-C (10%) in 100 ml dry ethanol were purged with N_2 and refluxed at 83 ℃. To this mixture, a solution of 17.5 ml of $N_2H_4 \cdot H_2O$ and 75ml ethanol was added dropwise and resulting mixture was refluxed for 12 hr. The mixture was filtered hot through a bed of celite and washed four times with 30 ml of boiling ethanol each time. The filtrate was dried over rotary evaporator and the residue was triturated with 50 ml of water and left at 4 ℃ overnight. The dark yellow coloured tan solid was washed thrice with cold water and dried in oven at 60 ℃ for 5 hr. The yellow solid was confirmed ^{1}H NMR, ^{13}C NMR, HRMS.

^{1}H NMR (500 MHz, DMSO) δ 8.77 (d, *J* = 3.3 Hz, 2H), 8.48 (d, *J* = 8.2 Hz, 2H), 7.61 (dd, *J* = 8.4, 4.2 Hz, 2H), 5.23 (s, 4H). **^{13}C NMR (101 MHz, DMSO)** δ 140.98, 129.78, 121.57, 118.65, 118.34, 114.06. **MS:** m/z: 211.0969 [$(M+H)^+$].

Synthesis of tCz-DPPN [2,3-bis(4-(3,6-di-tert-butyl-9H-carbazol-9-yl) phenyl) pyrazino[2,3-f] [1,10] phenanthroline]

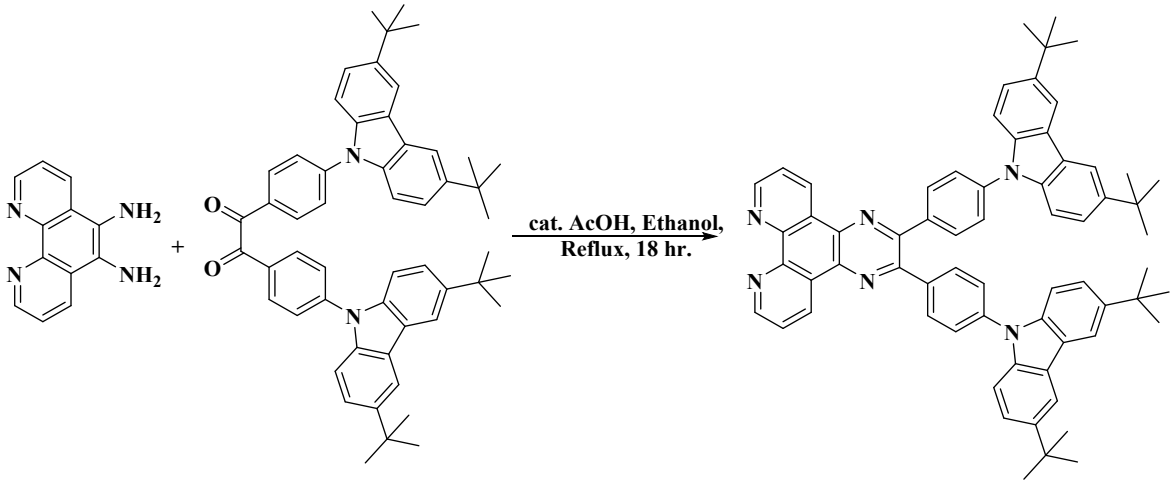

Scheme S2a. Synthesis of ***t*Cz-DPPN.**

The di-keto compound **2** [1,2-bis(4-(3,6-di-tert-butyl-9H-carbazol-9-yl) phenyl) ethane-1,2-dione] (800 mg, 1.0465 mmol) was dissolved in ethanol in presence of the catalytic amount of acetic acid, stirred for 30 mins. Afterward, 1,10 phenanthroline-5,6-diamine (220.016 mg, 1.0465 mmol) was dissolved in ethanol and added to the reaction mixture dropwise. The mixture was refluxed at 80^{o}C for 18 hr. After completion of the reaction, the excess ethanol was removed using rota-vapor. Solid product was extracted in dichloromethane and dried on Na_2SO_4. Pure product ***tCz*-DPPN** was obtained by column chromatography (2% MeOH in

DCM on 60-120 mesh silica gel) with a yield of 61.20%. Their chemical structures were confirmed by ^{1}H NMR, ^{13}C NMR, HRMS.

^{1}H NMR (500 MHz, $CDCl_3$) δ 9.69 (d, *J* = 7.4 Hz, 2H), 9.34 (d, 2H), 8.17 (s, 4H), 8.04 (d, *J* = 8.4 Hz, 4H), 7.87 (d, 2H), 7.73 (d, *J* = 8.4 Hz, 4H), 7.51 (s, 8H), 1.48 (s, 36H). **^{13}C NMR (126 MHz, $CDCl_3$) δ** 143.51, 139.53, 138.92, 136.87, 135.99, 131.76, 126.39, 123.97, 123.85, 116.52, 109.44, 77.16, 34.92, 32.15. **MS:** m/z: 939.5111[$(M+H)^+$].

Synthesis of Ac-DPPN [2,3-bis(4-(9,9-dimethylacridin-10(9H)-yl) phenyl) pyrazino[2,3-f] [1,10] phenanthroline]

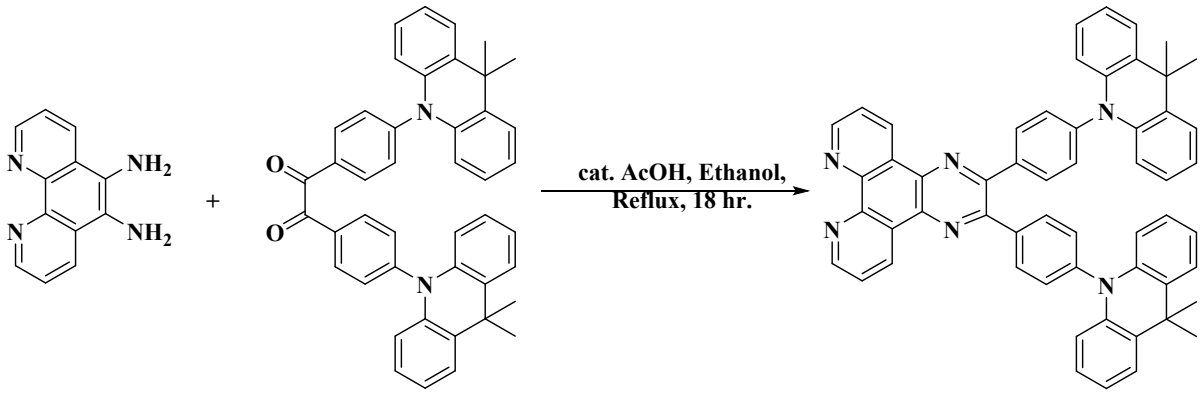

Scheme S2b. Synthesis of **Ac-DPPN.**

The di-keto compound **3** [1,2-bis(4-(9,9-dimethylacridin-10(9H)-yl) phenyl) ethane-1,2-dione] (800 mg, 1.2815 mmol) was dissolved in ethanol in presence of the catalytic amount of acetic acid, stirred for 30 mins. Afterward, 1,10 phenanthroline-5,6-diamine (269.422 mg, 1.2815 mmol) was dissolved in ethanol and added to the reaction mixture dropwise. The mixture was refluxed at 80^{o}C for 18 hr. After completion of the reaction, the excess ethanol was removed using rota-vapor. Solid product was extracted in dichloromethane and dried on Na_2SO_4. Pure product **Ac-DPPN** was obtained by column chromatography (2% MeOH in DCM on 60-120 mesh silica gel) with a yield of 56.06%. Their chemical structures were confirmed by ^{1}H NMR, ^{13}C NMR, HRMS.

^{1}H NMR (500 MHz, $CDCl_3$) δ 9.73 (d, *J* = 8.0 Hz, 2H), 9.40 (d, *J* = 2.8 Hz, 2H), 8.05 (d, *J* = 8.3 Hz, 4H), 7.91 (dd, *J* = 7.9, 4.3 Hz, 2H), 7.49 (d, *J* = 7.0 Hz, 8H), 7.00 – 6.89 (m, 8H), 6.42 (d, *J* = 9.3 Hz, 4H), 1.73 (s, 12H). **^{13}C NMR (101 MHz, $CDCl_3$)** δ 142.16, 140.50, 138.23, 133.29, 132.50, 131.23, 130.17, 126.34, 125.00, 123.93, 120.71, 113.85, 77.16, 35.87, 30.72. **MS:** m/z:799.3517 [$(M+H)^+$].

Synthesis of PXZ-DPPN [2,3-bis(4-(10H-phenoxazin-10-yl) phenyl) pyrazino[2,3-f] [1,10] phenanthroline]

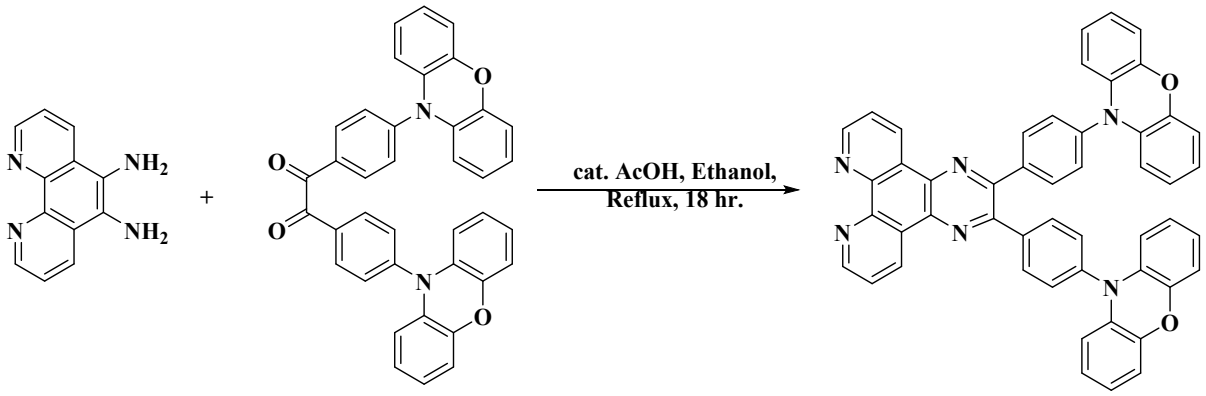

Scheme S2c. Synthesis of **PXZ-DPPN.**

The di-keto compound **4** [1,2-bis(4-(10H-phenoxazin-10-yl) phenyl) ethane-1,2-dione] (800 mg, 1.397 mmol) was dissolved in ethanol in the presence of the catalytic amount of acetic acid, stirred for 30 mins. Afterward, 1,10 phenanthroline-5,6-diamine (293.662 mg, 1.397 mmol) was dissolved in ethanol and added to the reaction mixture dropwise. The mixture was refluxed at 80^{o}C for 18 hr. After completion of the reaction, the excess ethanol was removed using rota-vapor. Solid product was extracted in dichloromethane and dried on Na_2SO_4. Pure product **PXZ-DPPN** was obtained by column chromatography (2% MeOH in DCM on 60-120 mesh silica gel) with a yield of 57.76%. Their chemical structures were confirmed by ^{1}H NMR, ^{13}C NMR, HRMS.

^{1}H NMR (500 MHz, $CDCl_3$) δ 9.68 (d, *J* = 7.8 Hz, 2H), 9.38 (s, 2H), 7.96 (d, *J* = 8.2 Hz, 2H), 7.89 (d, *J* = 4.6 Hz, 4H), 7.45 (d, *J* = 8.2 Hz, 4H), 6.72 (d, *J* = 6.8 Hz, 4H), 6.66 (t, *J* = 7.4 Hz, 4H), 6.57 (t, *J* = 7.6 Hz, 4H), 6.02 (d, *J* = 7.7 Hz, 4H). **^{13}C NMR (126 MHz, $CDCl_3$)** δ 143.87, 139.97, 139.95, 138.55, 133.82, 132.70, 130.84, 123.30, 121.57, 115.54, 113.03, 77.16. **MS:** m/z:747.2486 [$(M+H)^{+}$].

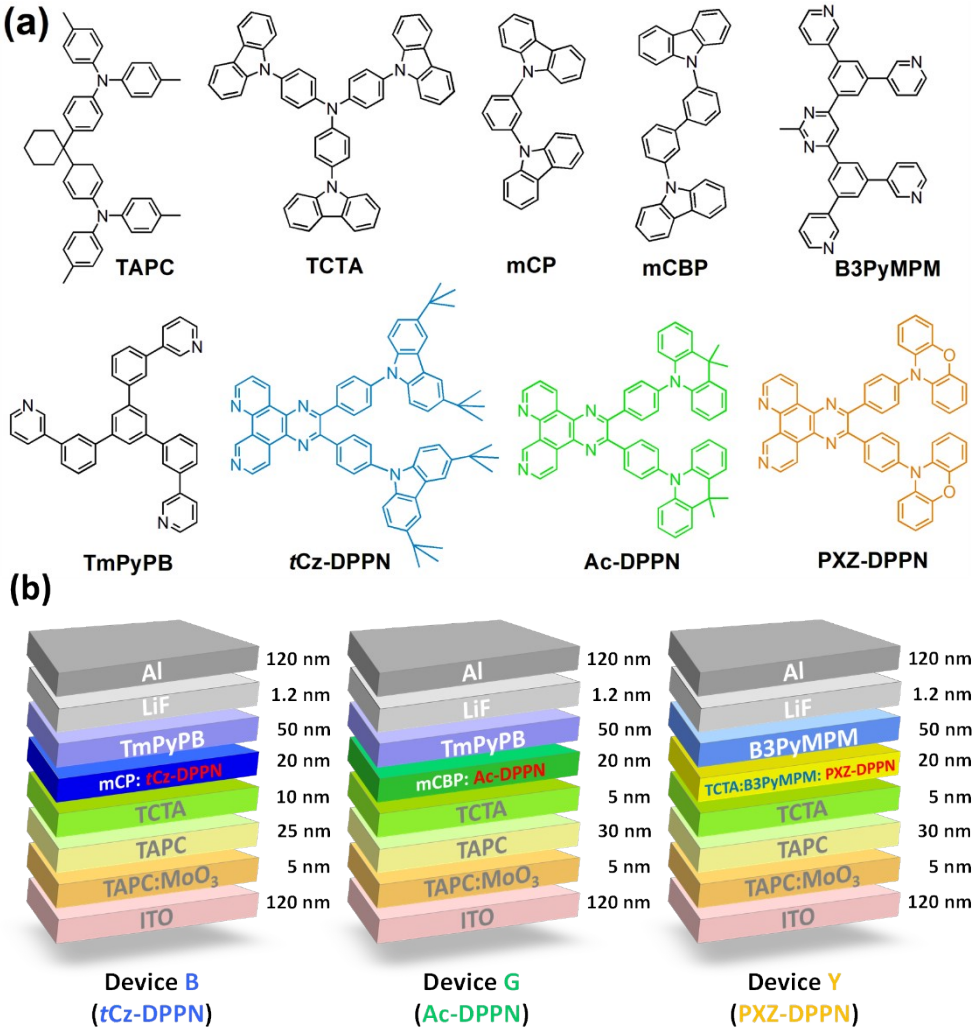

Figure S1. (a) Structural drawings of the materials used in OLEDs and (b) schematic structures of the fabricated OLEDs with different emitters.

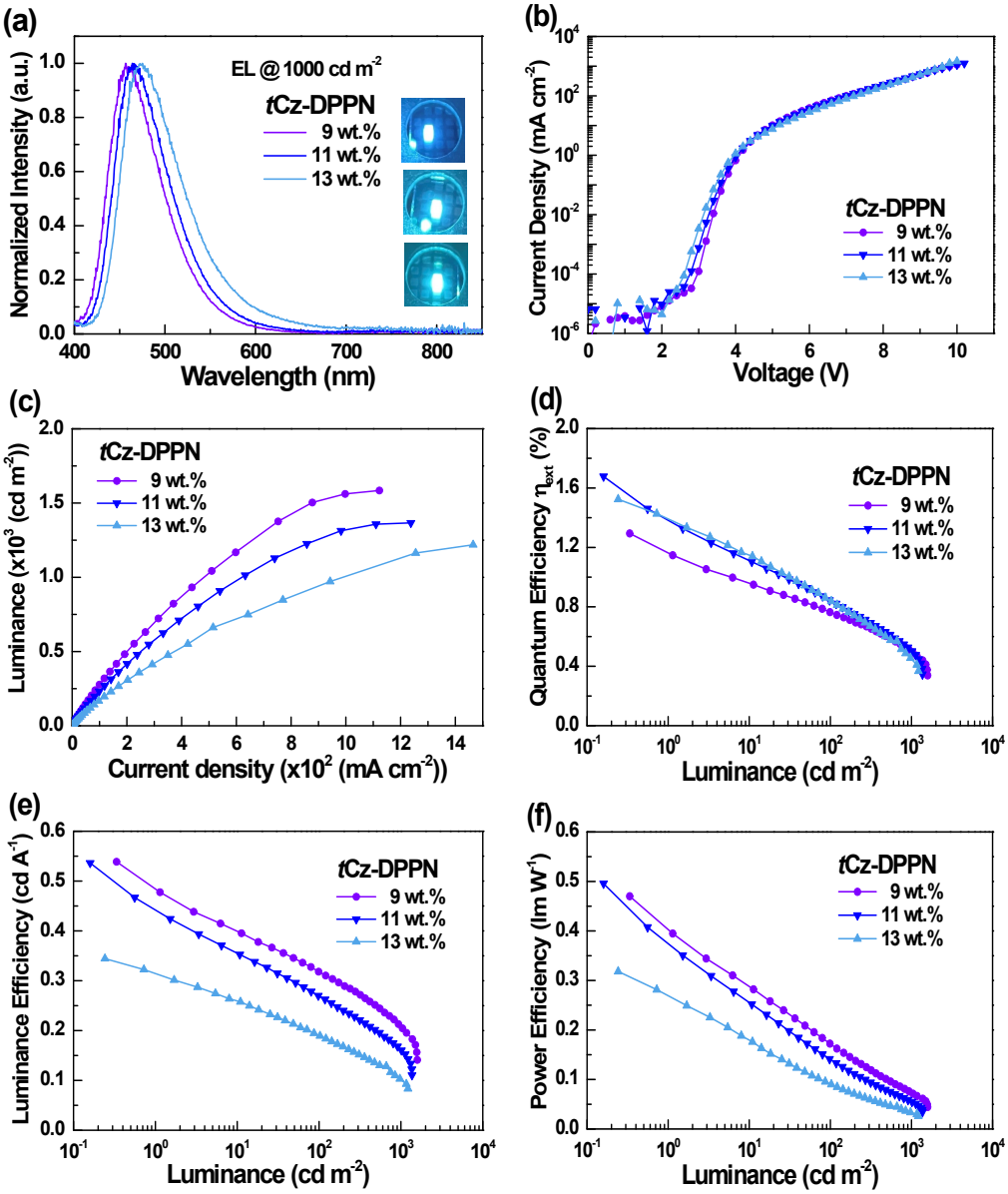

Figure S2. (a) Normalized EL spectra at a luminance of 1000 cd/m^2; (b) current density−voltage (J−V) characteristics; (c) luminance−current density (L−V) characteristics; (d) external quantum efficiency vs luminance; (e) luminance efficiency vs luminance; (f) power efficiency vs luminance for device B (***t*Cz-DPPN**) with different doping concentrations.

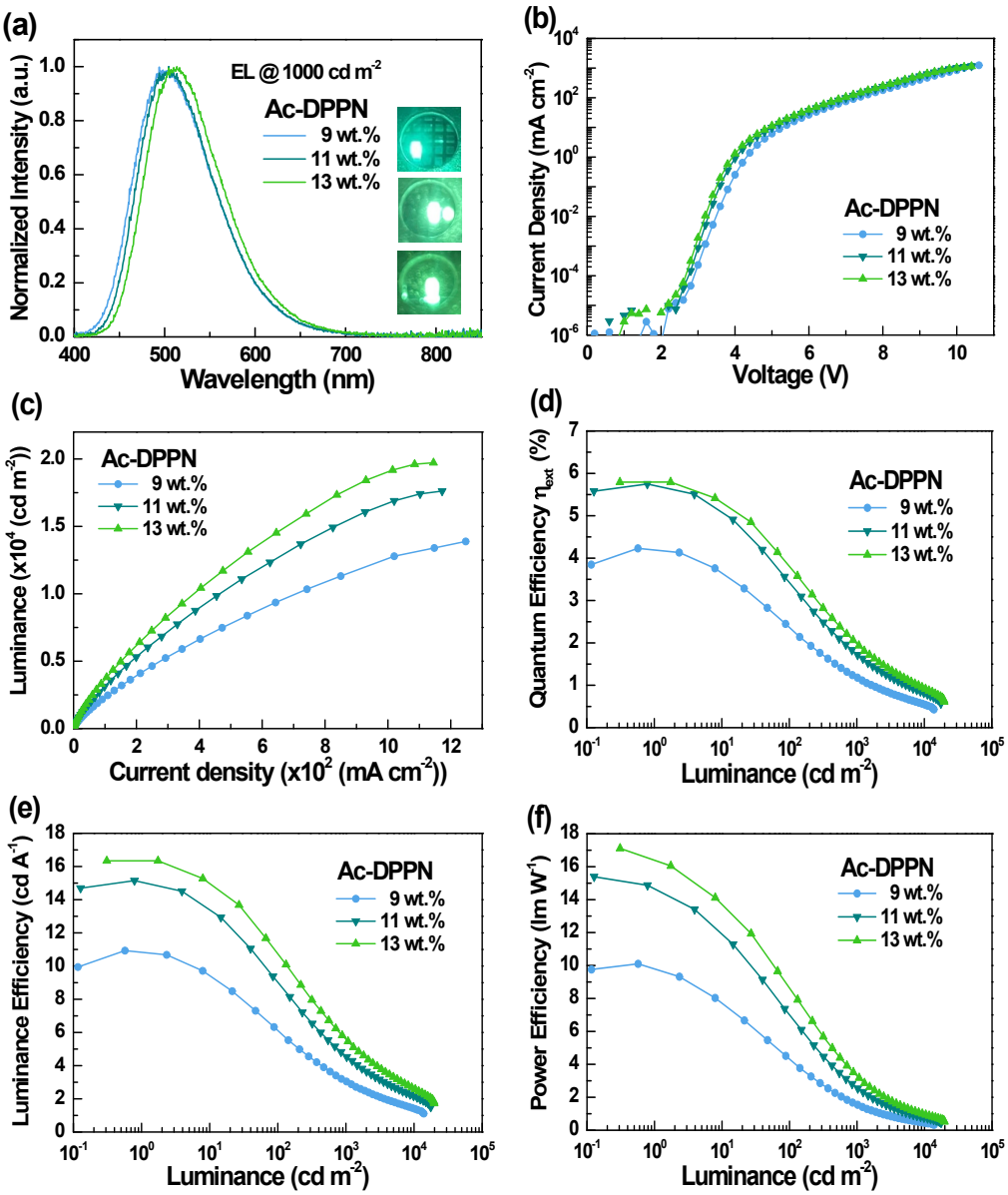

Figure S3. (a) Normalized EL spectra at a luminance of 1000 cd/m^2; (b) current density−voltage (J−V) characteristics; (c) luminance−current density (L−V) characteristics; (d) external quantum efficiency vs luminance; (e) luminance efficiency vs luminance; (f) power efficiency vs luminance for device G (**Ac-DPPN**) with different doping concentrations.

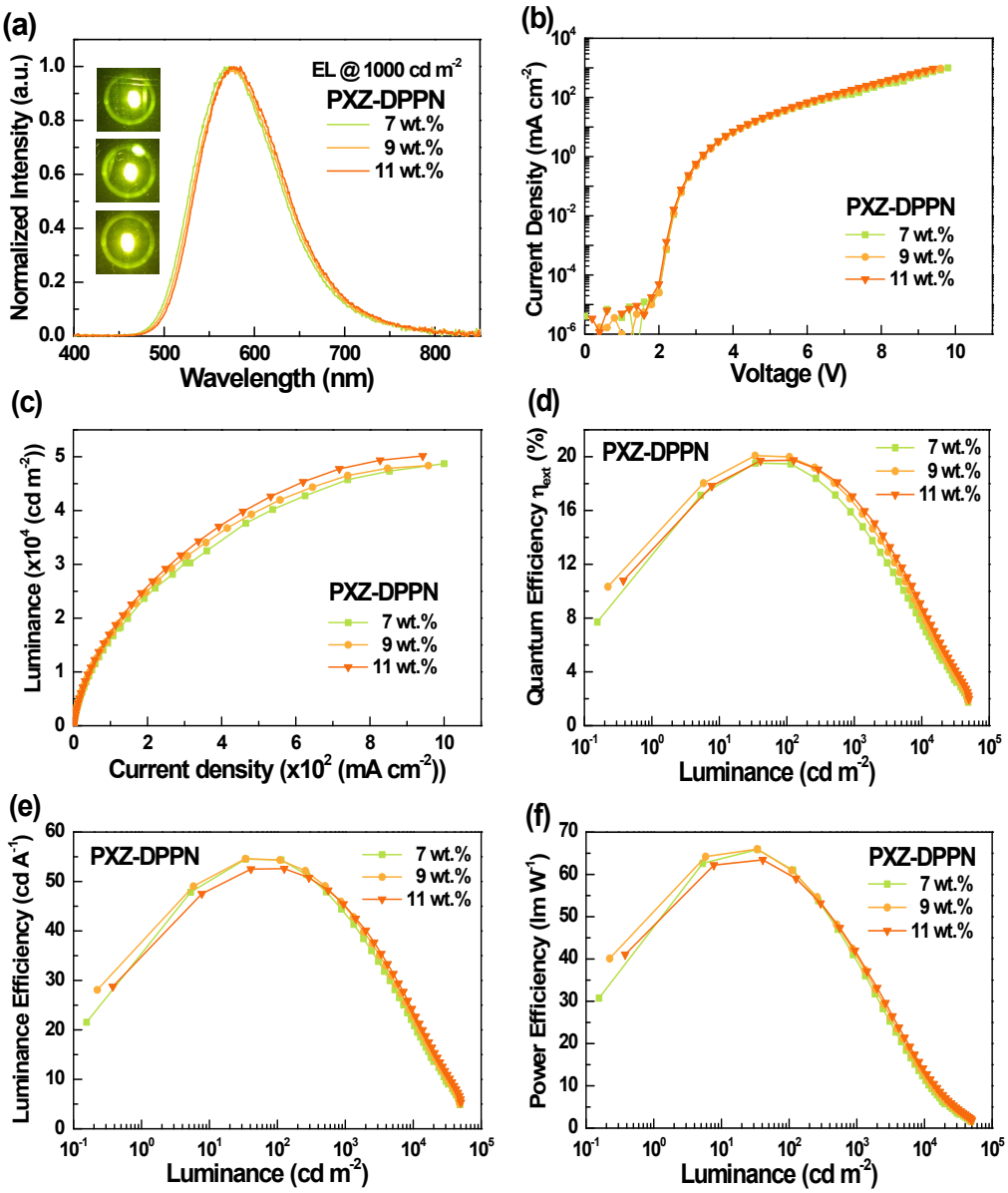

Figure S4. (a) Normalized EL spectra at a luminance of 1000 cd/m^2; (b) current density−voltage (J−V) characteristics; (c) luminance−current density (L−V) characteristics; (d) external quantum efficiency vs luminance; (e) luminance efficiency vs luminance; (f) power efficiency vs luminance for device Y (**PXZ-DPPN**) with different doping concentrations.

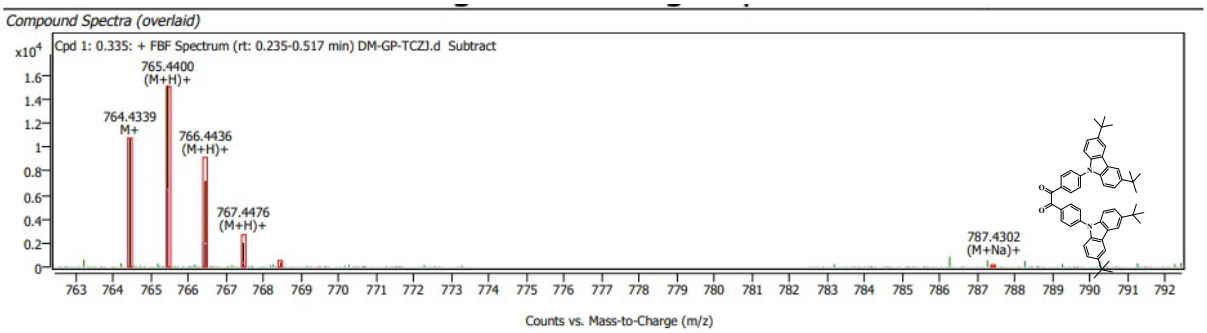

Figure S5. HRMS plot of [1,2-bis(4-(3,6-di-tert-butyl-9H-carbazol-9-yl) phenyl) ethane-1,2-dione] (**2**)

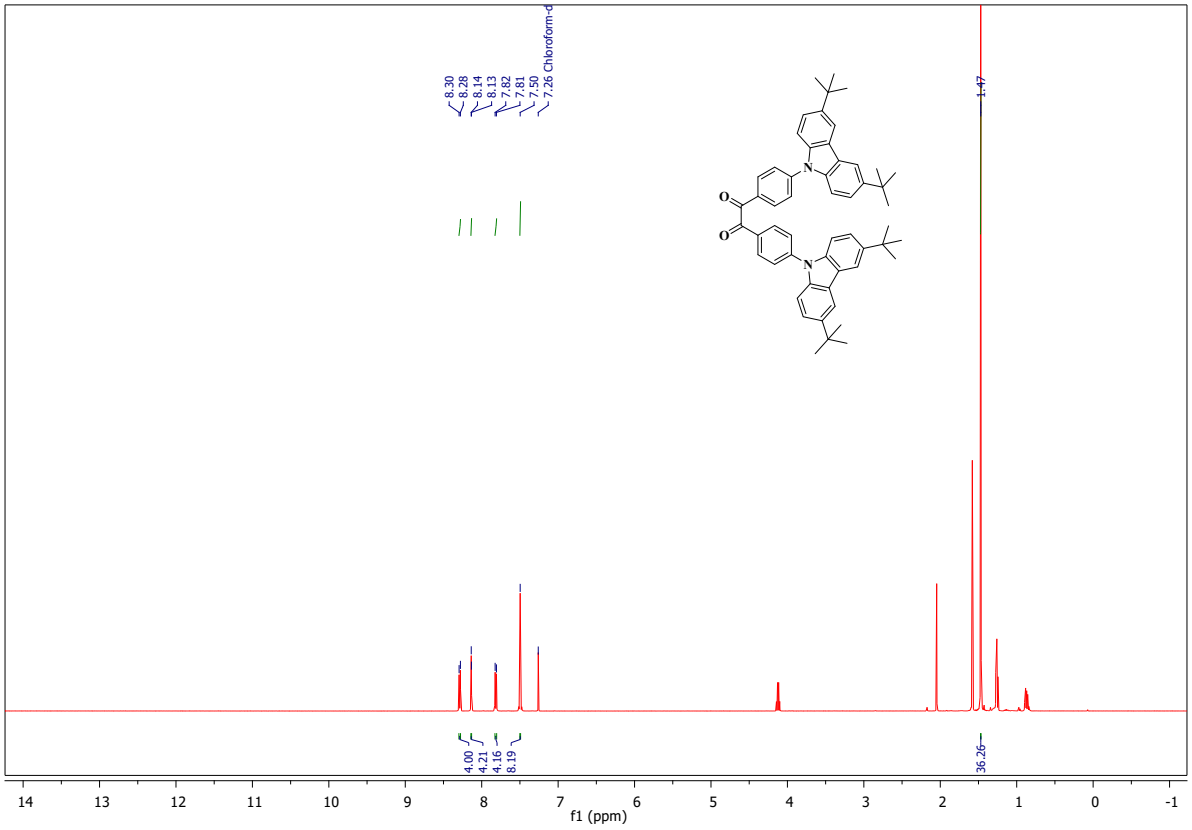

Figure S6. ^{1}H NMR plot of [1,2-bis(4-(3,6-di-tert-butyl-9H-carbazol-9-yl) phenyl) ethane-1,2-dione] (**2**)

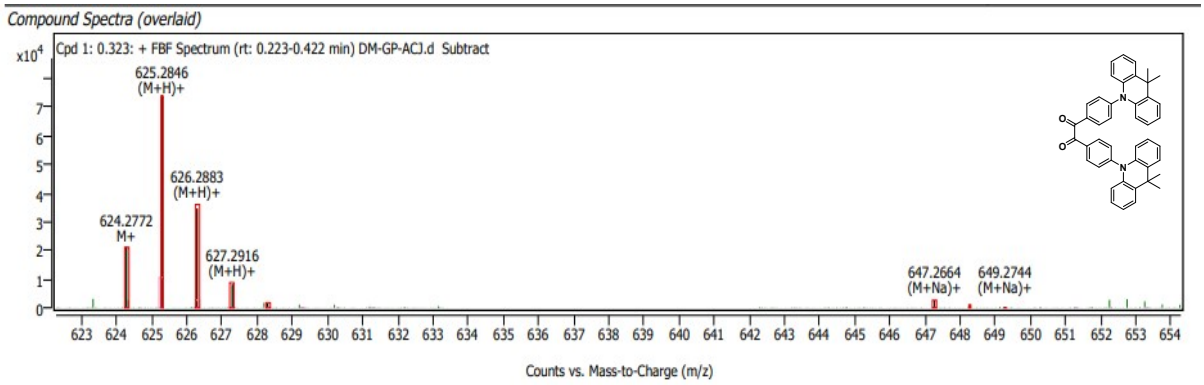

Figure S7. HRMS plot of [1,2-bis(4-(9,9-dimethylacridin-10(9H)-yl) phenyl) ethane-1,2-dione] **(3).**

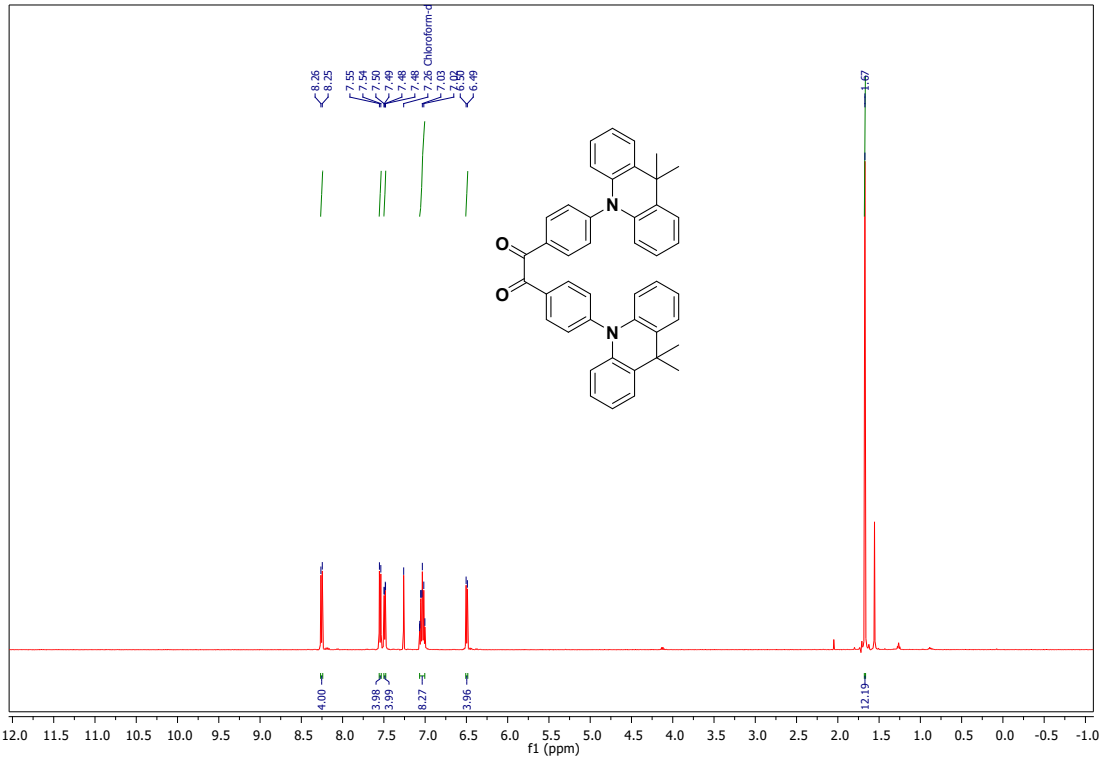

Figure S8. ^{1}H NMR plot of [1,2-bis(4-(9,9-dimethylacridin-10(9H)-yl) phenyl) ethane-1,2-dione] **(3).**

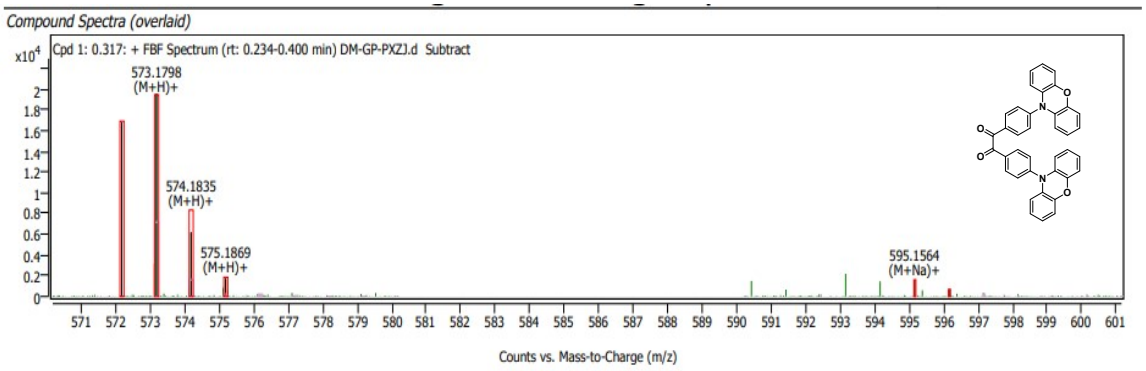

Figure S9. HRMS plot of [1,2-bis(4-(10H-phenoxazin-10-yl) phenyl) ethane-1,2-dione] **(4)**

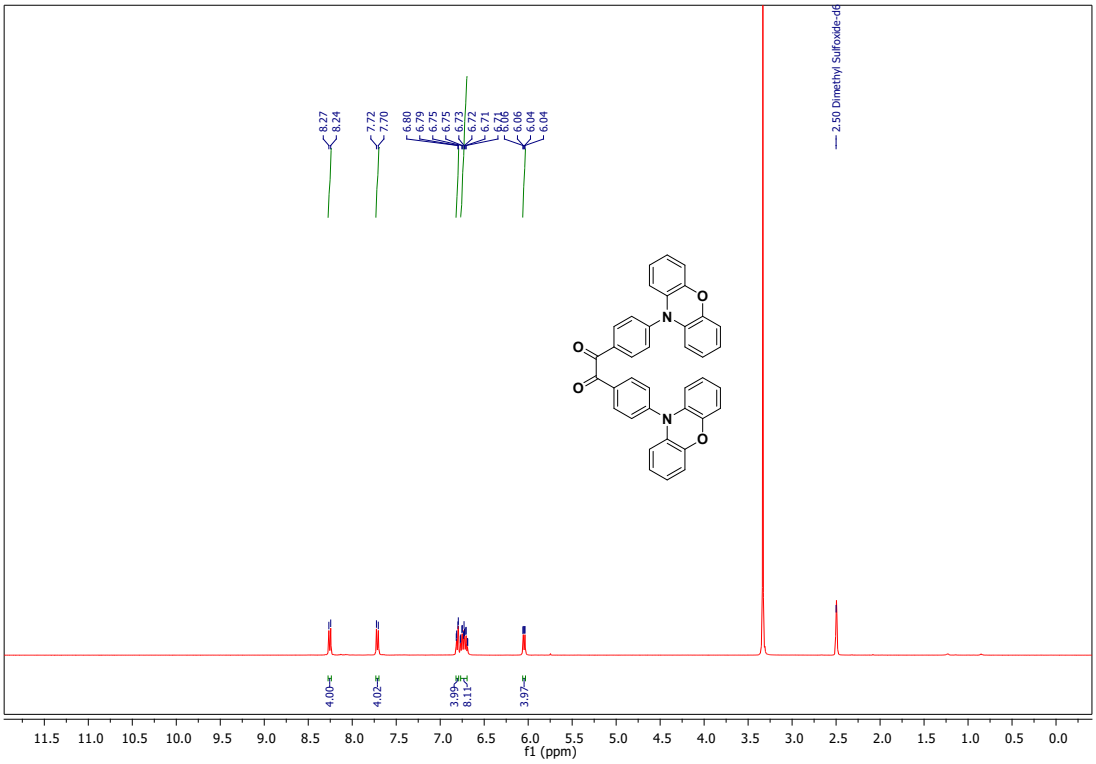

Figure S10. ^{1}H NMR of [1,2-bis(4-(10H-phenoxazin-10-yl) phenyl) ethane-1,2-dione] **(4).**

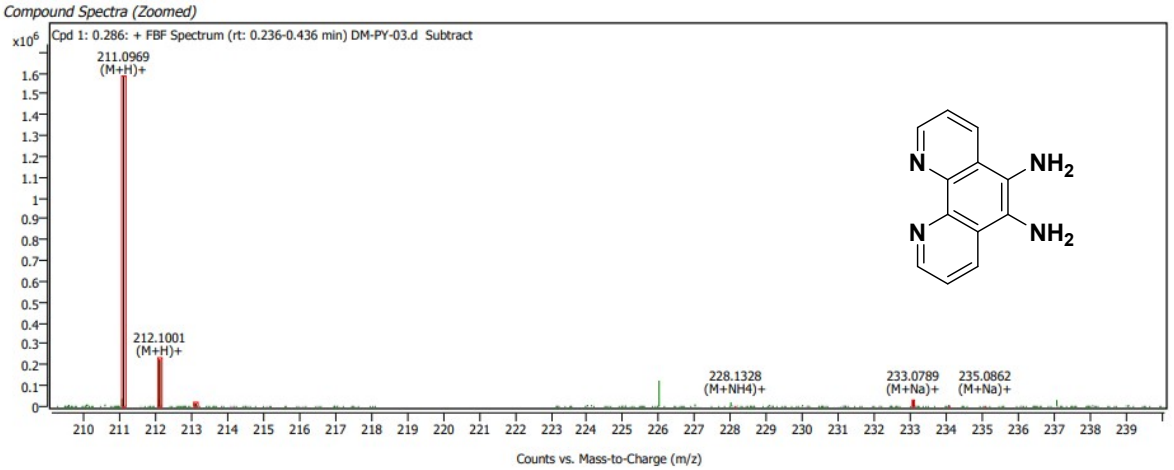

Figure S11. HRMS plot of 1,10 phenanthroline-5,6-diamine.

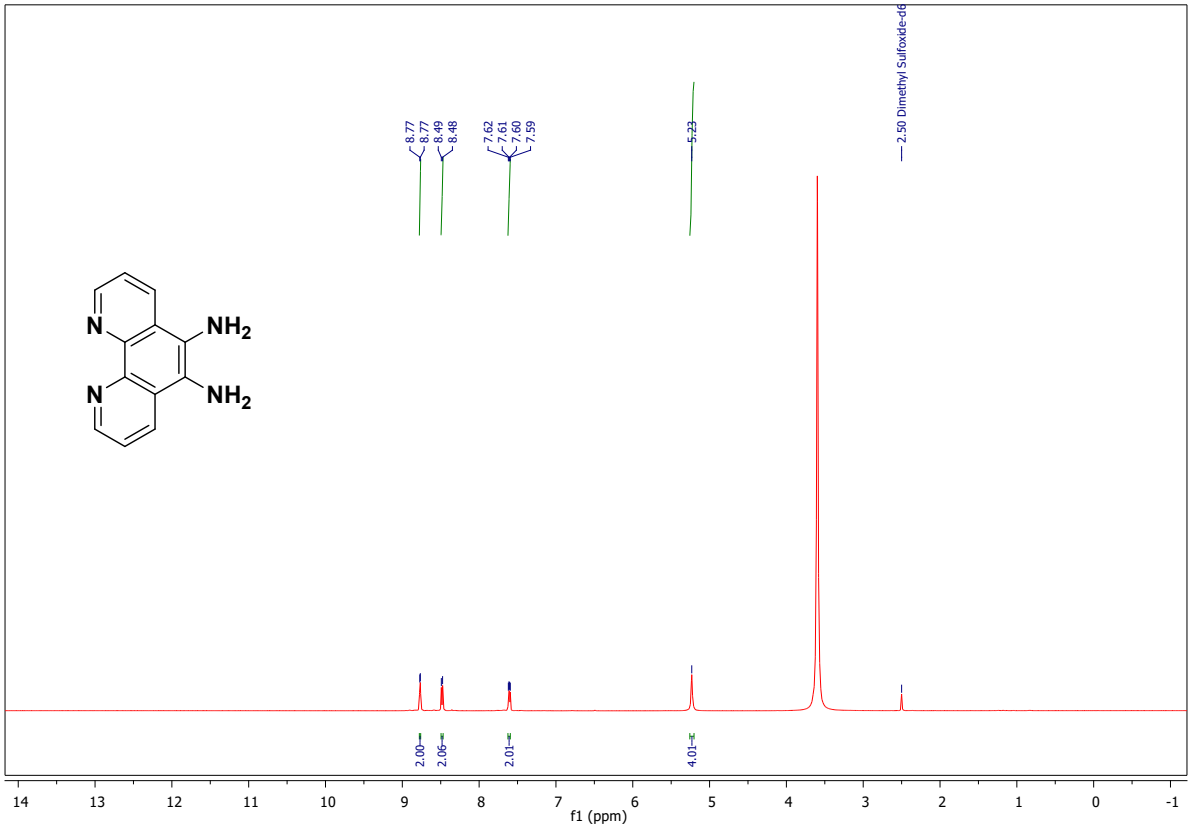

Figure S12. ^{1}H NMR plot of 1,10 phenanthroline-5,6-diamine.

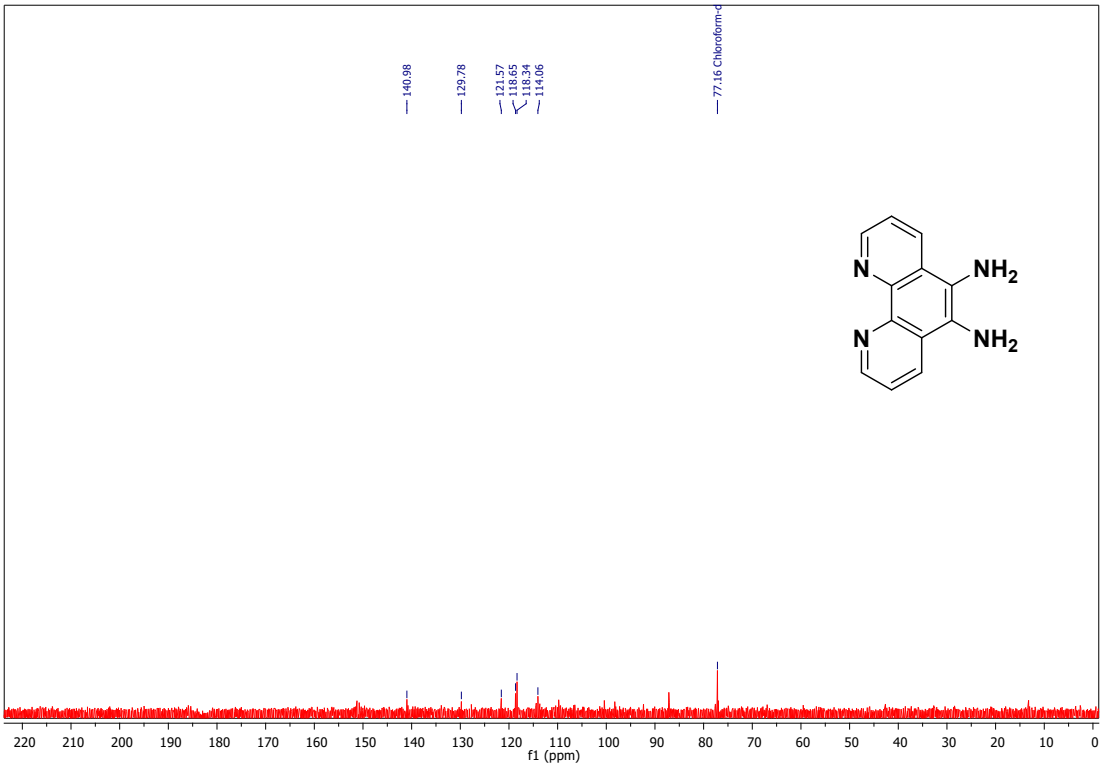

Figure S13. ^{13}C NMR plot of 1,10 phenanthroline-5,6-diamine.

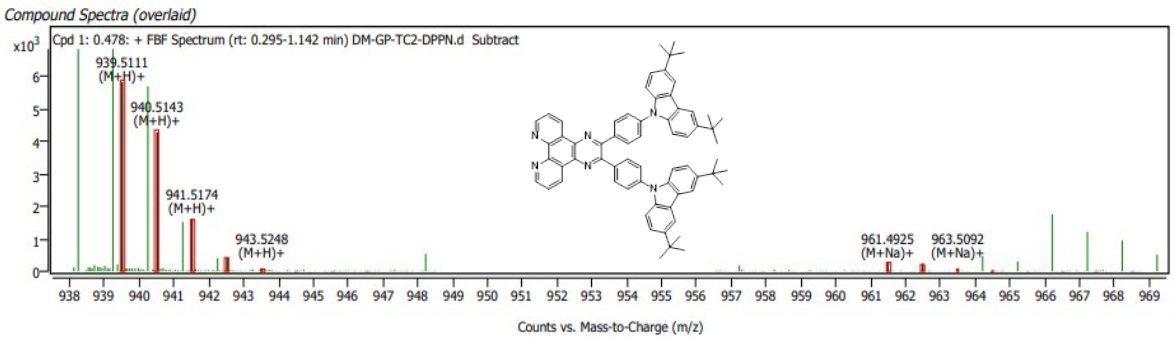

Figure S14. HRMS of [2,3-bis(4-(3,6-di-tert-butyl-9H-carbazol-9-yl)phenyl)pyrazino[2,3-f][1,10]phenanthroline] **(*t*Cz-DPPN).**

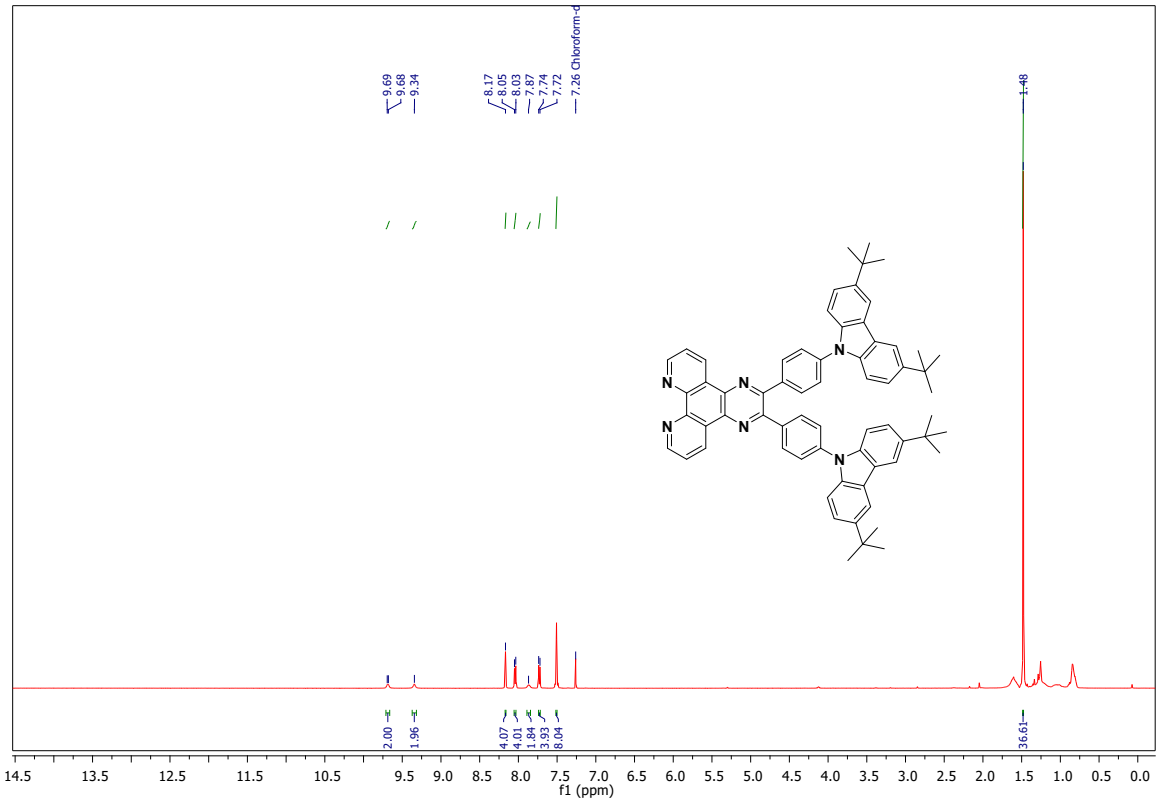

Figure S15. ^{1}H NMR plot of [2,3-bis(4-(3,6-di-tert-butyl-9H-carbazol-9-yl)phenyl) pyrazino[2,3-f][1,10]phenanthroline] **(*t*Cz-DPPN).**

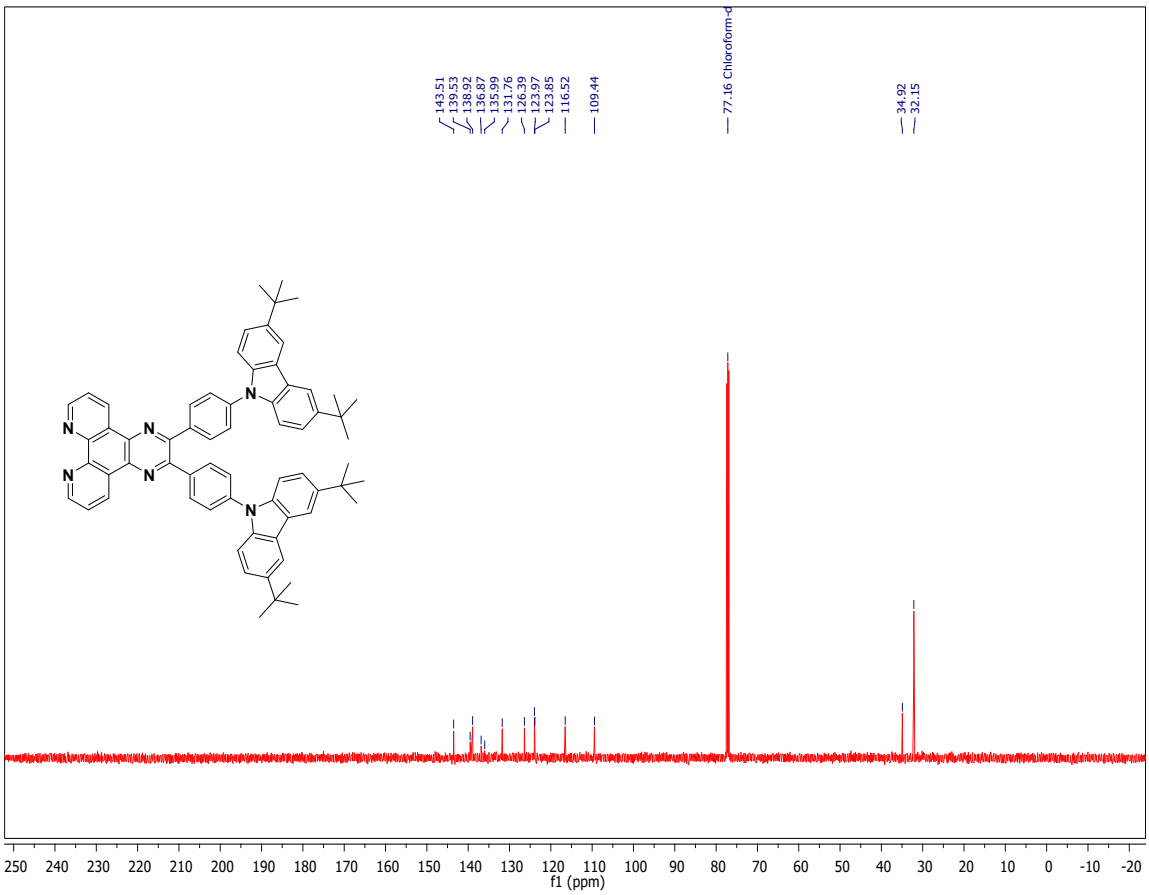

Fi

gure S16. ^{13}C NMR plot of [2,3-bis(4-(3,6-di-tert-butyl-9H-carbazol-9-yl) phenyl) pyrazino[2,3-f][1,10]phenanthroline] **(*t*Cz-DPPN).**

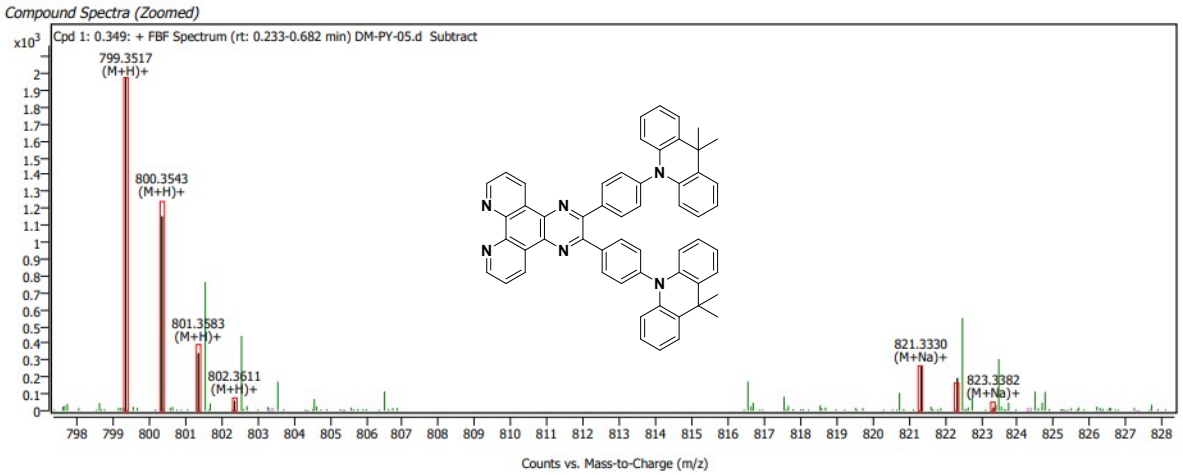

Figure S17. HRMS plot of [2,3-bis(4-(9,9-dimethylacridin-10(9H)-yl) phenyl) pyrazino[2,3-f] [1,10] phenanthroline] (**Ac-DPPN).**

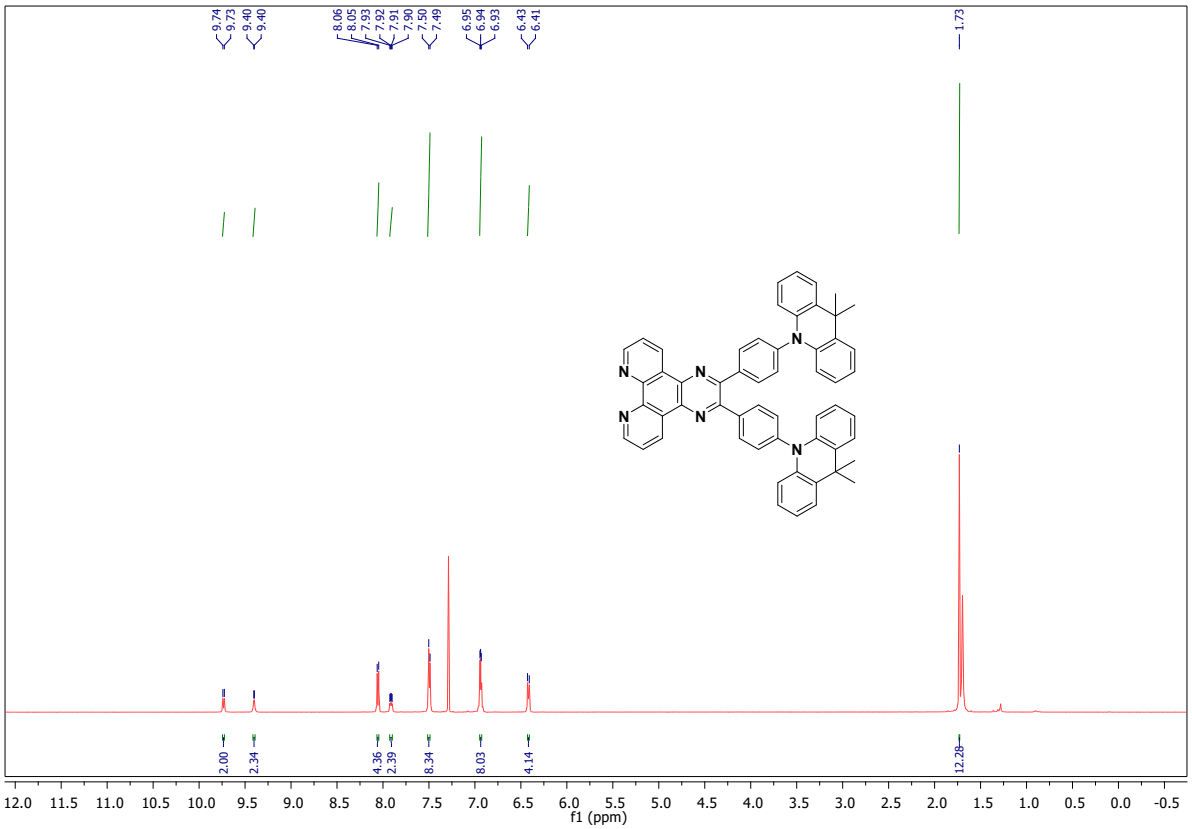

Figure S18. ^{1}H NMR plot of [2,3-bis(4-(9,9-dimethylacridin-10(9H)-yl) phenyl) pyrazino[2,3-f] [1,10] phenanthroline] (**Ac-DPPN).**

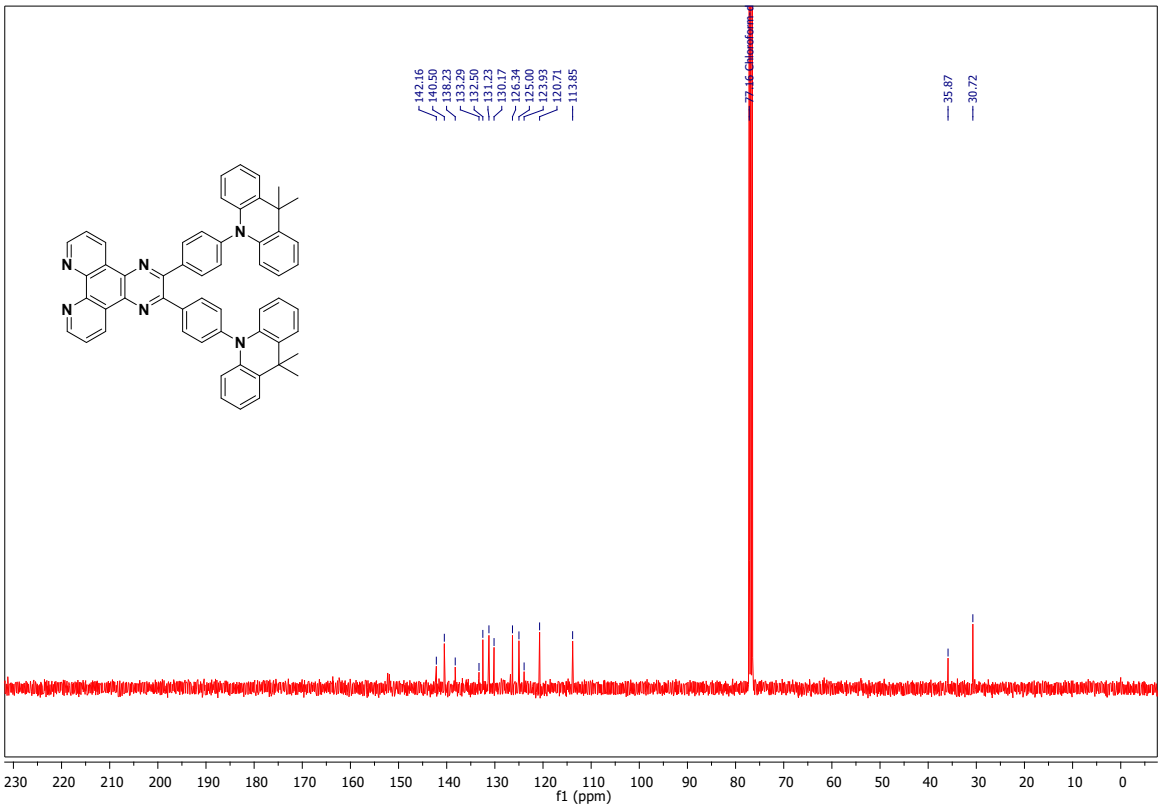

Figure S19. ^{13}C NMR plot of [2,3-bis(4-(9,9-dimethylacridin-10(9H)-yl) phenyl) pyrazino[2,3-f] [1,10] phenanthroline] (**Ac-DPPN).**

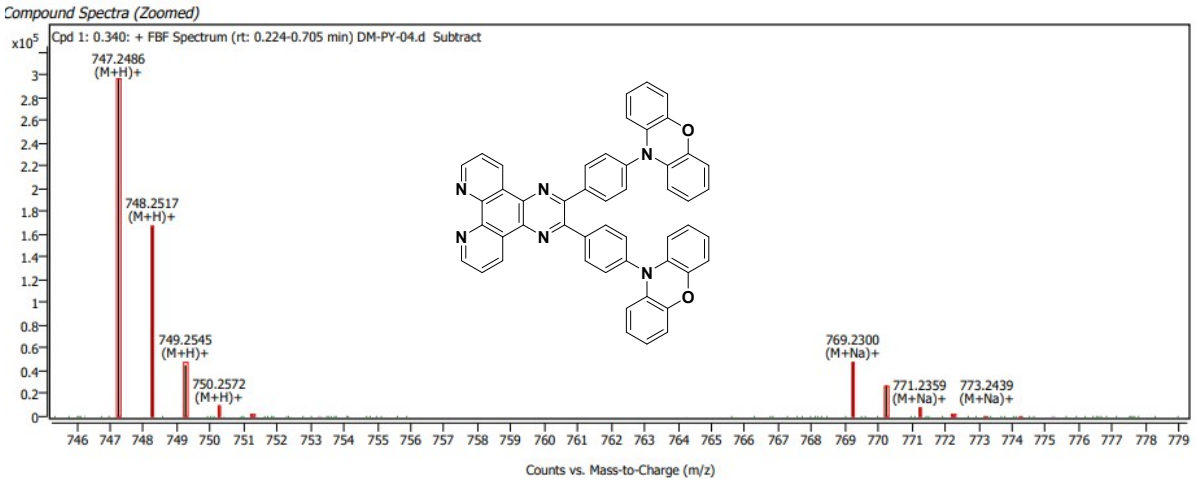

Figure S20. HRMS plot of [2,3-bis(4-(10H-phenoxazin-10-yl) phenyl) pyrazino[2,3-f] [1,10] phenanthroline] **(PXZ-DPPN).**

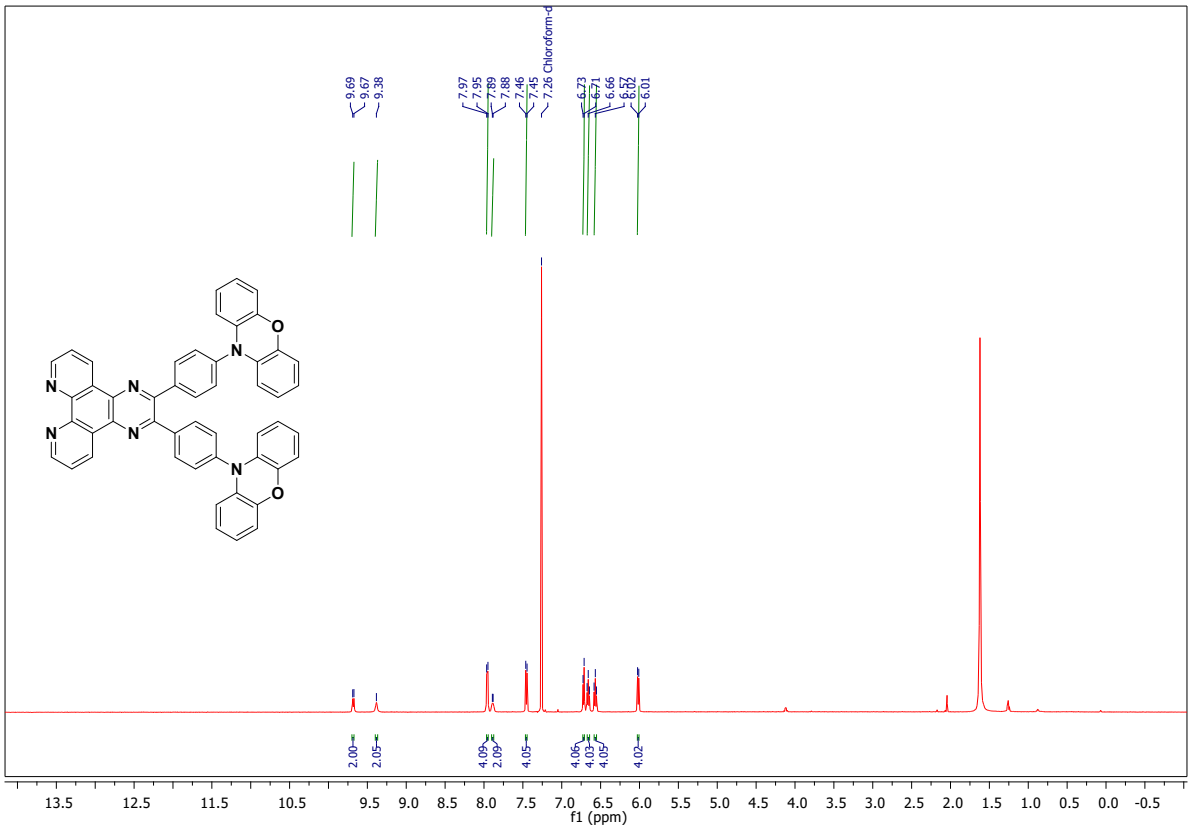

Figure S21. ^{1}H NMR plot of [2,3-bis(4-(10H-phenoxazin-10-yl) phenyl) pyrazino[2,3-f] [1,10] phenanthroline] **(PXZ-DPPN).**

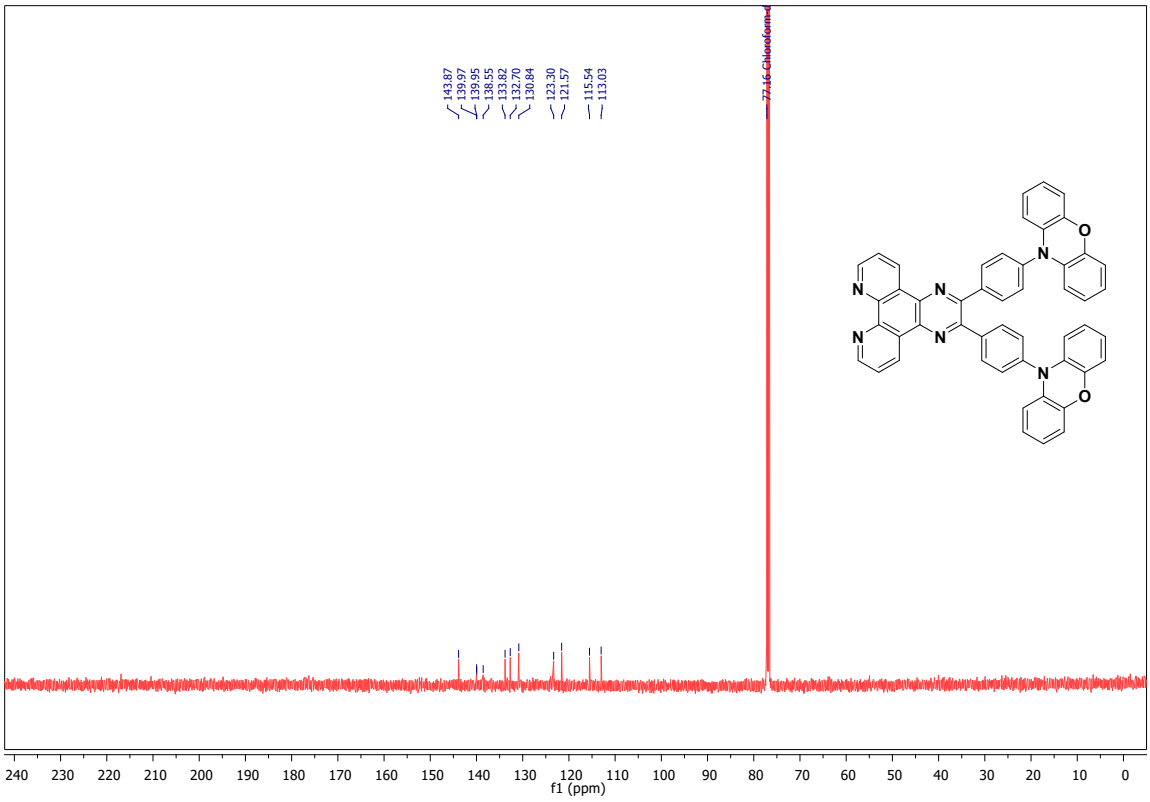

Figure S22. ^{13}C NMR of [2,3-bis(4-(10H-phenoxazin-10-yl) phenyl) pyrazino[2,3-f] [1,10] phenanthroline] **(PXZ-DPPN).**

Theoretical studies: Computational studies were conducted to validate experimental results by using the Gaussian 16 quantum mechanical software package for DFT (Density Functional Theory) and TDDFT (Time Dependent Density Functional Theory) computations.

Table S1. Optimized structures of synthesized molecules at B3LYP/6-31+G (d, p) level of theory.

Molecules	Optimized Structures
***t*Cz-DPPN**	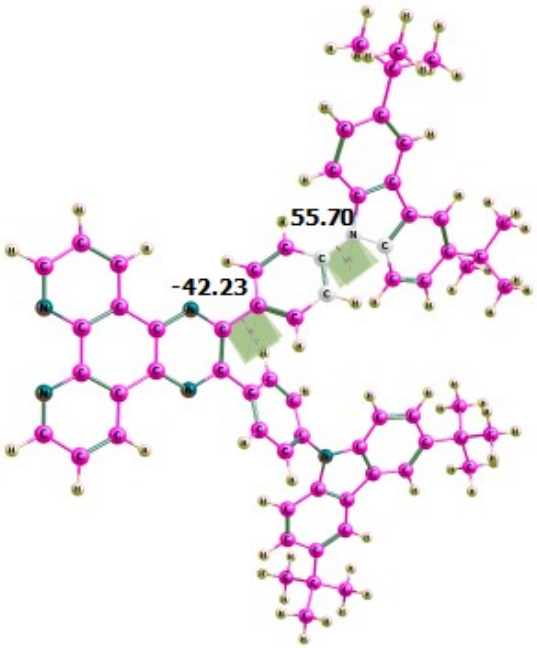
Ac-DPPN	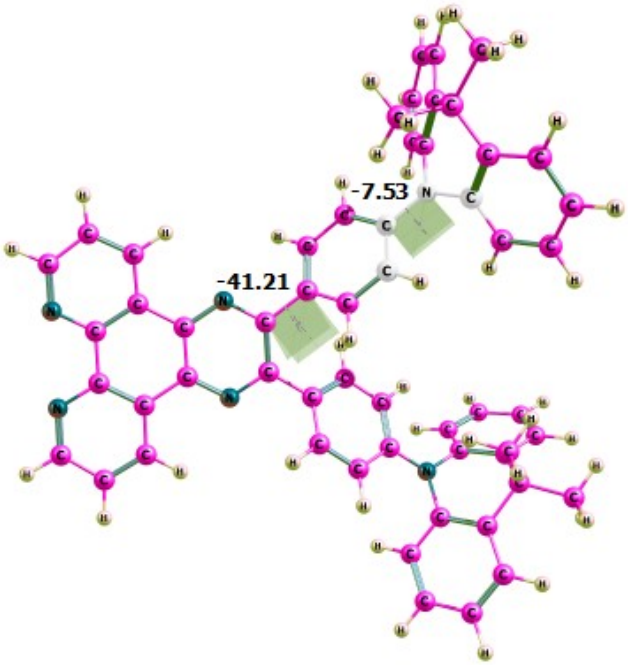

PXZ-DPPN	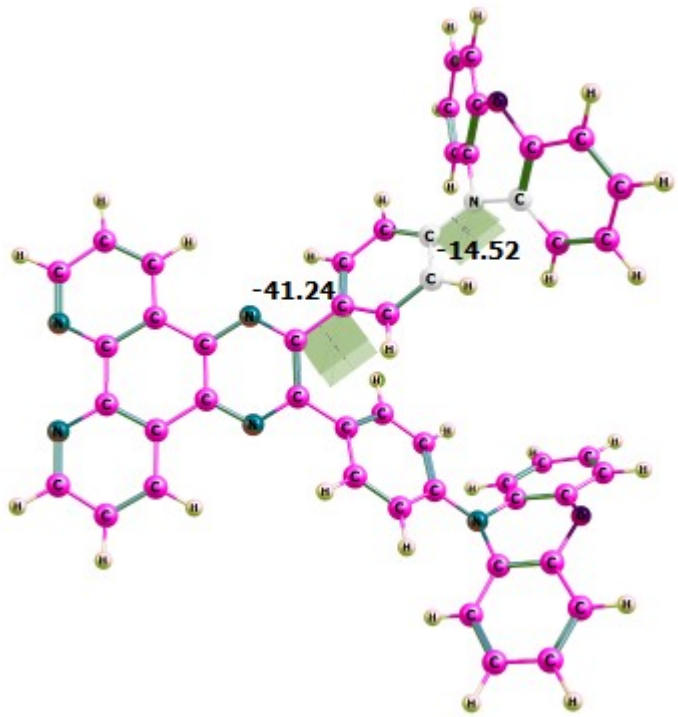

Table S2. Calculated Absorption, Oscillator strength, Molecular transitions and % contribution at TD-DFT/CAM-B3LYP/6-31+G (d, p) level.

Molecule	States	Absorption	*f*	M.T.	%Ci
***t*Cz-DPPN**	S1	357	0.645	H-4 → L	42
				H → L	41
	S2	326	0.1536	H-4 → L	16
				H-4 → L+1	10
				H-1 → L	35
				H → L+1	19
	S3	311	0.0215	H-16 → L	27
				H-12 → L	18
				H-5 → L	14
	S4	307	0.1493	H-16 → L	15
				H-12 → L	11
				H-4 → L	11
				H-1 → L+1	11
				H → L+1	18
	S5	303	0.1015	H-4 → L	10
				H-1 → L	36
				H → L	36
Ac-DPPN	S1	376	0.6803	H-2 → L	11
				H → L	83

	S2	335	0.501	H-1 → L	21
				H → L+1	55
	S3	308	0.0022	H-16 → L	33
				H-15 → L	14
				H-14 → L	17
				H-1 → L	11
	S4	300	0.0778	H-1 → L	53
				H → L+1	20
	S5	292	0.4546	H-3 → L+1	15
				H-1 → L+1	36
PXZ-DPPN	S1	344	0.6953	H-2 → L	11
				H → L	80
	S2	322	0.5074	H → L+1	67
	S3	305	0.0048	H-10 → L	14
				H-9 → L	21
				H-8 → L	33
	S4	286	0.41	H-3 → L+1	17
				H-1 → L+1	25
				H → L+2	10
	S5	280	0.0092	H-1 → L	43
				H → L+1	12

Table S3. Population analysis of molecular orbitals for the synthesized molecules at B3LYP/6-31+G (d, p) level of theory

Molecules	**Molecular orbitals**	
***t*Cz-DPPN**	HOMO-1 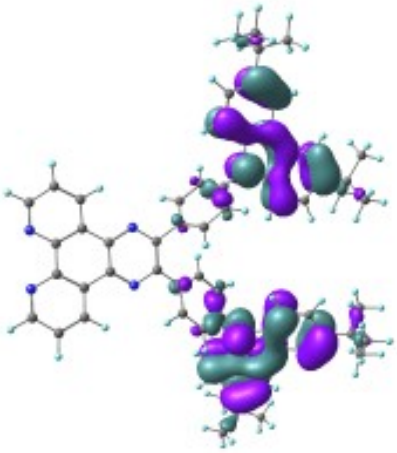	LUMO+1 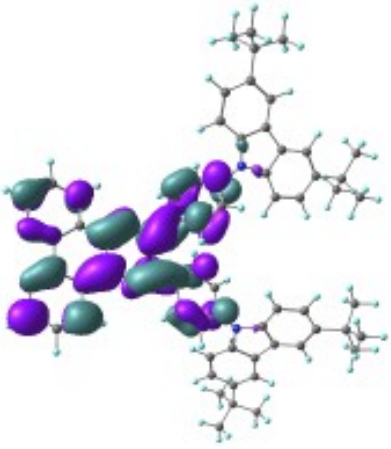
	HOMO -2	LUMO +2

	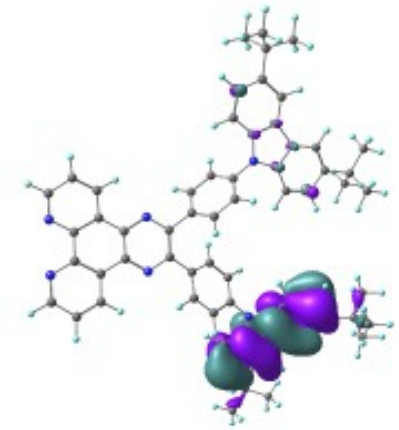	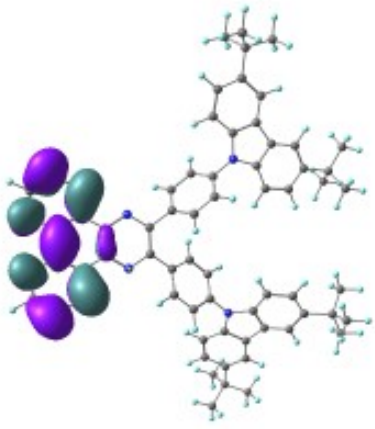
Ac-DPPN	HOMO-1 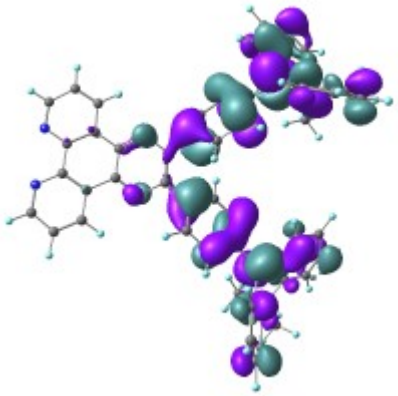	LUMO+1 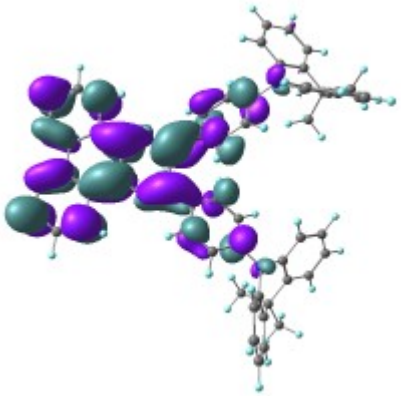
	HOMO-2 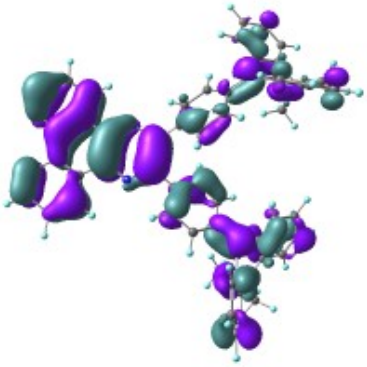	LUMO+2 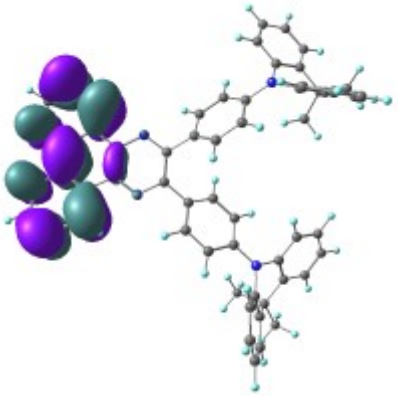

PXZ-DPPN	HOMO-1 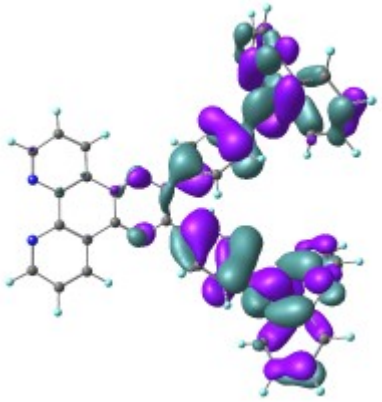	LUMO+1 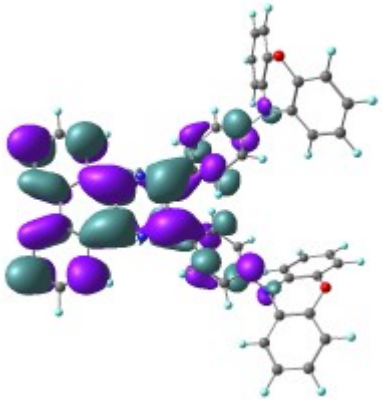
	HOMO-2 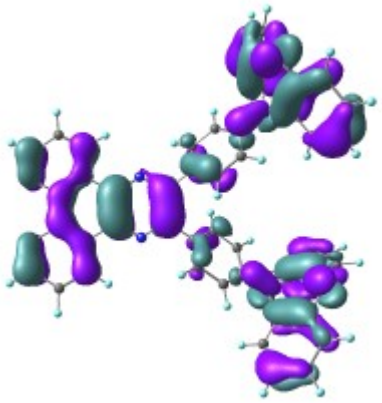	LUMO+2 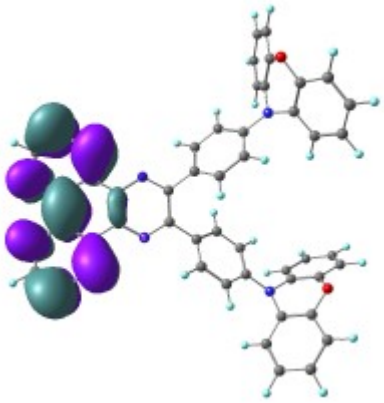

Table S4. Molecular Electrostatic Potentials for the synthesized molecules.

Molecules	Molecular Electrostatic Potentials
***t*Cz-DPPN**	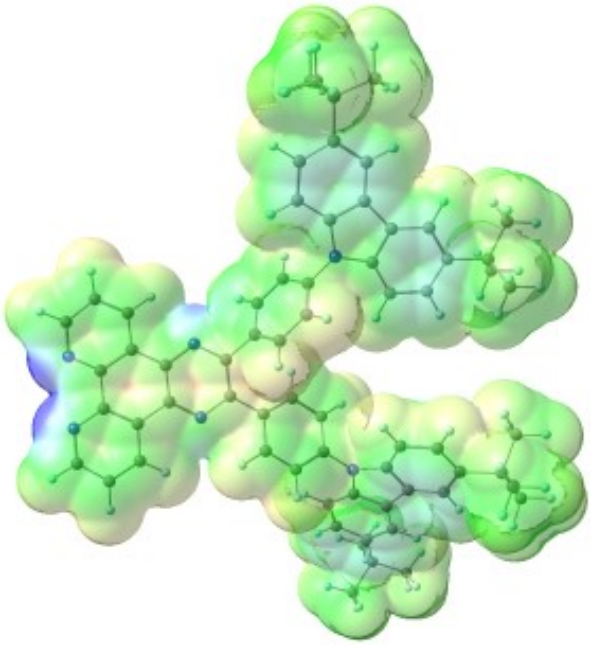

Ac-DPPN	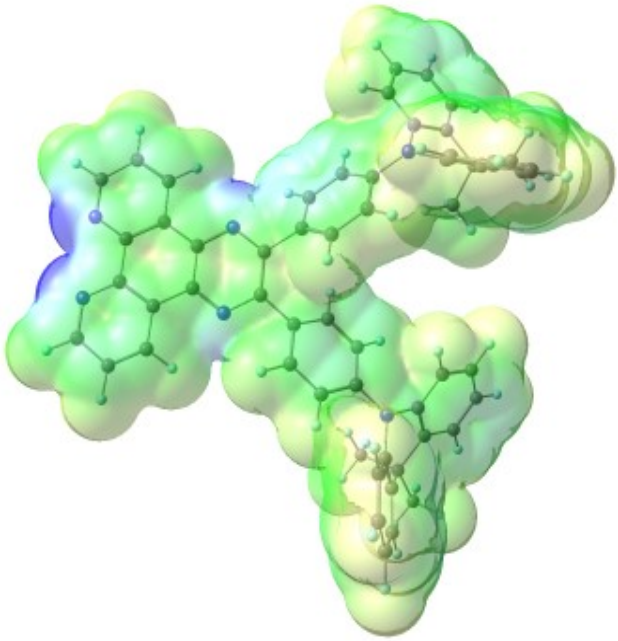
PXZ-DPPN